SUPPLEMENTAL MATERIALS

KLF4-dependent perivascular plasticity contributes to adipose tissue inflammation

Gamze B. Bulut Ph.D.[1], Gabriel F. Alencar Ph.D.[1], Katherine M. Owsiany[1], Anh T. Nguyen Ph.D.[1], Santosh Karnewar Ph.D.[1], Ryan M. Haskins Ph.D.[1], Lillian K. Waller[1], Olga A. Cherepanova Ph.D.[2], Rebecca A. Deaton Ph.D.[1], Laura S. Shankman, Ph.D.[1], Susanna R. Keller, M.D.[3] and Gary K. Owens Ph.D.[1]

[1] The Robert M. Berne Cardiovascular Research Center, University of Virginia
[2] Cardiovascular and Metabolic Sciences Lerner Research Institute, Cleveland Clinic
[3] Department of Medicine-Division of Endocrinology and Metabolism, University of Virginia

Short title: Perivascular plasticity and adipose tissue inflammation

Corresponding Author:
Gary K. Owens, Ph.D.
gko@virginia.edu
415 Lane Road PO Box 801394
University of Virginia School of Medicine
Charlottesville, VA 22908
434-924-2652

SUPPLEMENTAL FIGURE LEGENDS

Supplemental Figure I: Myh11-eYFP$^+$ MΦ marker$^+$ cells from adipose tissue comprise approximately 5% of adipose MΦs and exhibit M2 polarization. Epididymal adipose tissue SVF cells were prepared for flow cytometry, as described in **Figure 1E**, except that mice were switched to DIO diet for 4 weeks at 10 weeks of age. (**A**) Gating strategy for flow cytometry. The percentage of eYFP positive cells were identified within total the MΦ marker, CD45, positive cells. This method showed that only ~5% of adipose tissue CD45$^+$ cells are present in the eYFP$^+$ gate. (**B** and **C**) *Myh11*-Cre^{ERT2}eYFP mice received 10 tamoxifen injections in peanut oil between 6 – 8 weeks of age, followed by a 2-week washout period. The mice were fed a normal diet or DIO diet for 6 weeks before tissues were harvested. Body weights (**B**) and adipose tissue weights (**C**) of mice receiving either normal diet or DIO diet were plotted (Mean ± SEM). Data indicate that *Myh11*-Cre^{ERT2}eYFP mice responded to the high fat diet as expected. For (**B**) *P* values were determined using unpaired two-tailed *t*-test with Welch's correction. For (**C**) *P* values were determined using an ordinary Two-way ANOVA with alpha = 0.05 followed by Sidak's multiple comparisons post-test. (**D**) M1 versus M2 MΦ classification was done by co-staining cells for CD86 and CD206. About 40% of eYFP$^+$ MΦ marker$^+$ cells also express CD206 and exhibit M2 MΦ polarization. AT: adipose tissue. Epi: Epididymal adipose tissue, Subcu: Subcutaneous adipose tissue, Mes: Mesenteric adipose tissue.

Supplemental Figure II: Gating strategy applied for flow sorting of cells from *Myh11*-Cre^{ERT2}eYFP mice for single-cell RNA sequencing. Representative flow cytometry plots. Viability-dye negative cells were gated to exclude dead cells. FSC-A versus SSC-A gating was applied to exclude debris. Subsequently, FSC-H versus FSC-A gating was applied to exclude doublets. The eYFP FMO gate was set using epididymal adipose tissue SVF cells from a *Myh11*-Cre^{ERT2}eYFP control mouse not given IP tamoxifen in peanut oil. Four experimental groups were analyzed: *Myh11*-Cre^{ERT2}eYFP SMC-P lineage-tracing mice on normal diet (Group 1, N.D.), or 6 weeks DIO diet (Group 2, "DIO"), as well as SMC-P *Klf4*$^{WT/WT}$ on DIO diet (SMC-P *Klf4*$^{WT/WT}$ DIO, Group 3), and SMC-P *Klf4*$^{\Delta/\Delta}$ on DIO diet (SMC-P *Klf4*$^{\Delta/\Delta}$ DIO, Group 4) for 6 weeks. For each experimental group, epididymal SVF cells were sorted for four cell-type groups, including eYFP$^+$CD45$^-$, eYFP$^+$CD45$^+$CD11b$^+$F4/80$^+$ (eYFP$^+$ MΦ), eYFP$^-$ CD45$^+$CD11b$^+$F4/80$^+$ (eYFP$^-$ MΦ), and eYFP$^-$CD45$^-$ cells followed by scRNA-seq library preparation resulting in a total of 16 libraries. For each sample, 2000 cells were targeted with 50,000 reads/cell. A total of 25,356 total cells were analyzed including: N.D. (4,516 cells), DIO (3,995 cells), SMC-P *Klf4*$^{WT/WT}$ DIO (8,506 cells), SMC-P *Klf4*$^{\Delta/\Delta}$ DIO (8,339 cells). N.D. diet dataset flow sorting plots are shown.

Supplemental Figure III: *Myh11*-Dre^{ERT2}tdTom lineage tracing system validation. (**A** and **B**) *Myh11*-Dre$^{ERT2+/-}$tdTom (Dre^{pos}) or *Myh11*-Dre$^{ERT2-/-}$tdTom (Dre^{neg}) mice were injected (Tmx. Inj) or not injected (Non-tmx. Inj) with tamoxifen between 6 - 8 weeks of age, and various tissues were harvested at 9 weeks of age for immunostaining with an anti-tdTomato antibody or IgG isotype control. (**A**) *Myh11*-Dre$^{ERT2+/-}$tdTom but not negative control mice treated with tamoxifen show efficient labeling of the

brachiocephalic artery (BCA). (**B**) Quantification of single cell-counting from immunostained BCA regions using confocal microscopy for $tdTom^{+}/DAPI^{+}$ cells (mean ± SEM) indicating >92% labeling efficiency. *P* values were determined using unpaired two-tailed *t*-test with Welch's correction; n = 8 for *Myh11*-$Dre^{ERT2+/-}$tdTom mice treated with tamoxifen, n = 3 for *Myh11*-$Dre^{ERT2-/-}$tdTom treated with tamoxifen, and n = 4 for *Myh11*-$Dre^{ERT2+/-}$tdTom non-treated with tamoxifen. (**C**) Microvasculature of the liver stained with an anti-tdTomato antibody or IgG isotype control along with an ACTA2-FITC antibody. Pictures show maximum intensity projections of 10 μm confocal z-stacks. Non-tamoxifen injected control, as well as Dre negative tamoxifen injected BCA and liver counterstained with DAPI, were negative for tdTomato staining. Scale bars = 100 um. (**D**) Microvascular vessels of the retina from *Myh11*-$Dre^{ERT2+/-}$tdTom and *Myh11*-$Dre^{ERT2-/-}$tdTom mice were stained with ACTA2-FITC and imaged for ACTA2 and endogenous tdTomato signal. Results showed high efficiency and SMC-P specific tdTomato labeling of arteries, arterioles, and capillaries. Scale bars =100 μm (**E**) Aortas were harvested for flow cytometry from *Myh11*-$Dre^{ERT2+/-}$tdTom and *Myh11*-$Dre^{ERT2+/-}$tdTom mice treated with tamoxifen in the diet. Representative flow cytometry plots after gating out dead cells, debris, and doublets illustrating tdTomato positive cells. (**F**) Quantification of the percentage of SMC-P in aortas from *Myh11*-$Dre^{ERT2+/-}$tdTom or *Myh11*-$Cre^{ERT2+/-}$eYFP mice treated with tamoxifen via injections in peanut oil (Inj) or diet (Diet) based on flow cytometry. Values represent mean ± SEM. *P* values were determined using an ordinary Two-way ANOVA with alpha = 0.05 followed by Sidak's multiple comparisons post-test. *Myh11*-$Cre^{ERT2+/-}$eYFP (n = 6 Inj; n = 6 Diet); *Myh11*-$Dre^{ERT2+/-}$tdTom (n = 6 Inj; n = 10 Diet).

Supplemental Figure IV: Peanut oil injections do not result in changes in circulating cytokines. *Myh11*-Cre^{ERT2}eYFP mice received a series of tamoxifen injections in peanut oil for 10 days or were fed tamoxifen diet in normal diet followed by a 2-week standard normal diet, after which blood was harvested for a Luminex assay. Values represent mean ± SEM. *P* values were determined using an ordinary Two-way ANOVA with alpha = 0.05 followed by Sidak's multiple comparisons post-test. Tamoxifen injection group n = 7, tamoxifen diet group n = 5.

Supplemental Figure V: Gating strategy applied for flow sorting of cells from *Myh11*-Dre^{ERT2}tdTom lineage-tracing mice treated with tamoxifen in diet for single-cell RNA sequencing. Representative flow cytometry plots for both N.D. (*upper panels*) and DIO diet (*bottom panels*) fed mice. Viability-dye negative cells were gated to exclude dead cells. Subsequently, FSC-H versus FSC-A gating was applied to exclude doublets. The tdTomato FMO gate was set using epididymal adipose tissue SVF cells from a *Myh11*-$Dre^{ERT2+/-}$tdTom lineage tracing control mouse fed a normal diet without tamoxifen. The mice were fed either a normal diet or DIO diet for 6 weeks and then tissues were harvested. Two libraries were prepared for each condition: flow-sorted tdTomato positive cells or unsorted SVF cells resulting in 4 libraries. For each sample, 2000 cells were targeted with 50,000 reads per cell.

Supplemental Figure VI: SMC-P *Klf4*$^{\Delta/\Delta}$ mice are not resistant to diet-induced obesity, and do not display changes in circulating blood cell types, cytokines or

MΦ marker$^+$ cells in adipose tissue. SMC-P *Klf4*$^{WT/WT}$ and SMC-P *Klf4*$^{\Delta/\Delta}$ mice were injected with tamoxifen in peanut oil and fed DIO diet for indicated times (W – weeks). (**A**) Graphs of body weight measurements at the time of tissue harvest comparing SMC-P *Klf4*$^{WT/WT}$ and SMC-P *Klf4*$^{\Delta/\Delta}$ mice. (**B** and **C**) Blood cells (**B**) or epididymal adipose tissue SVF cell suspensions (**C**) from SMC-P *Klf4*$^{WT/WT}$ and SMC-P *Klf4*$^{\Delta/\Delta}$ mice after six weeks of DIO diet feeding were stained for flow cytometry. (**B**) Circulating blood cell types were gated as follows: live/singlets/scatter gates were initially applied to remove dead cells, doublets and debris. CD45$^+$ cells were gated for either CD4 or CD8 cells (excluding double negatives), then frequency of CD4 or CD8 single positive cells plotted. From the same CD45$^+$ gate, CD11b$^+$ cells were gated and then the frequency of Ly6c^{hi} monocytes and Ly6G$^+$ neutrophils plotted. CD19$^+$ out of CD45$^+$ cells were also plotted. (**C**) The percentage of CD45$^+$ cells among live/singlets and MΦ marker positive sub-populations showed no difference between genotypes. (**D**) Adipocyte size analysis was performed using Adipocount[39] on Hematoxylin and Eosin stained sections of epididymal adipose tissue samples. Representative images of sections from SMC-P *Klf4*$^{WT/WT}$ (n=11) and SMC-P *Klf4*$^{\Delta/\Delta}$ mice (n=11) are depicted. Scale bar is 100 um. The frequency distribution of adipocyte diameter across bins are plotted. *P* value is not significant using a Two-Way ANOVA comparing genotypes. (**E**) SMC-P *Klf4*$^{WT/WT}$ and SMC-P *Klf4*$^{\Delta/\Delta}$ mice received a series of tamoxifen injections in peanut oil for 10 days and subsequently fed DIO diet for six weeks, after which blood was harvested for a Luminex assay. Values represent mean ± SEM. SMC-P *Klf4*$^{WT/WT}$ n = 7, SMC-P *Klf4*$^{\Delta/\Delta}$ mice n = 6. (**F**) The abundance of crown like structures (CLS) were quantified manually using Hematoxylin and Eosin stained sections of epididymal adipose tissue samples from SMC-P *Klf4*$^{WT/WT}$ (n=12) and SMC-P *Klf4*$^{\Delta/\Delta}$ mice (n=12). The total number of CLS were divided by the number of sections analyzed per mouse. (**G**) Total RNA was isolated from epididymal adipose tissue samples using SMC-P *Klf4*$^{WT/WT}$ and SMC-P *Klf4*$^{\Delta/\Delta}$ mice and RT-PCR experiments were performed, normalizing the expression of genes to GAPDH. The sequences of all primers used are presented in Supplemental Table 2. Statistical Analysis for (**B**, **C**, **E**, **G**) Values show mean ± SEM. *P* values were determined using an ordinary Two-way ANOVA with alpha = 0.05 followed by Sidak's multiple comparisons post-test.

Supplemental Figure VII: eYFP transcript detection-based analysis confirmed that perivascular-specific loss of *Klf4* altered transcriptomic clustering of MΦs and lymphatic endothelial cells. (**A**) Schematic of experimental design. Single-cell RNAseq datasets for SMC-P *Klf4*$^{WT/WT}$ and SMC-P *Klf4*$^{\Delta/\Delta}$ mice fed a DIO diet for six weeks (see **Figure 2** for details) were subjected to eYFP transcript detection. After quality control of scRNAseq reads, alignment of reads was performed using the cell ranger software (10x Genomics) against a modified mouse mm10 genome that included a custom eYFP chromosome. For *in silico* correction, eYFP transcript negative cells were removed from eYFP positive flow-sorted libraries and vice versa. (**B**) Dot plot analysis depicting the expression levels and percentages of cells expressing a pre-determined list of traditional marker genes in each cluster. C) *Left Panel* - Color-coded UMAP plot for integrated libraries based on eYFP transcript detection depicting 25

clusters. *Middle Panel* - UMAP showing cell origins based on library preparation. *Right Panel* - Feature plot of *eYFP* transcript distribution. (**D**) UMAP plots comparing cells from SMC-P *Klf4*$^{WT/WT}$ (*left panel*) and SMC-P *Klf4*$^{\Delta/\Delta}$ (*middle panel*) mice. *Right panel* shows a feature plot for *Lyve1*, one of the top significantly differentially expressed genes for cluster 13. (**E** and **F**) Quantification of the frequency distribution of cells within each cluster from indicated libraries. (**G**) SMC-P *Klf4*$^{WT/WT}$ and SMC-P *Klf4*$^{\Delta/\Delta}$ mice were labeled with tamoxifen between 6 and 8 weeks of age, and after a 2-week washout period and following six week of DIO diet feeding epididymal adipose tissues were harvested for immunostaining with an anti-LYVE1 antibody. 10 um thick paraffin embedded sections were also co-stained with ACTA2-FITC and DAPI. Confocal z-stack images were acquired on Zeiss 880 microscope and analyzed for LYVE1^{+} vessel area. In brief, LYVE1^{+} vessel area was manually identified and quantified using Image J. The outline of the LYVE1^{+} vessels were drawn as a region of interest and Image J was used to calculate the area measurement after setting the scale using the scale bar measurement. Only structures representing sectioned vessels were included and statistical outliers were excluded from analysis. 1 to 3 sections were analyzed per animal from SMC-P *Klf4*$^{WT/WT}$ (n = 8) and SMC-P *Klf4*$^{\Delta/\Delta}$ mice (n = 10). An unpaired *t*-test with Welch's correction yielded $P = 0.0302$.

Supplemental Figure VIII: Histological analysis of adipose tissue sections from SMC-P *Klf4*$^{WT/WT}$ and SMC-P *Klf4*$^{\Delta/\Delta}$ mice reveal changes in ACTA2+ vessel area but no changes in CD31+ cells. (**A**) SMC-P *Klf4*$^{WT/WT}$ and SMC-P *Klf4*$^{\Delta/\Delta}$ mice were labeled with tamoxifen between 6 and 8 weeks of age, and after a 2-week washout period and following six week of DIO diet feeding epididymal adipose tissues were harvested for immunostaining with an anti-CD31 antibody (**A**) or IgG isotype control, or anti-LYVE1 antibody (**D**) or isotype control. Sections were also co-stained with ACTA2-FITC and DAPI. Confocal z-stack images were acquired on a Zeiss 880 microscope and analyzed for pixellation using Image J. Representative images of sections are depicted. Scale bar is 100 um. (**B, C**) Maximum intensity projections were generated using 5 sections for each z-stack and integrated density measurements were obtained using Image J, after defining a region of interest using the DIC image. The integrated density of CD31 pixellation was normalized to IgG controls and plotted as mean ± SEM. Similar to LYVE1+ vessel area, measurement of ACTA2+ vessel area was quantified using Image J. For both plots, an unpaired *t*-test with Welch's correction was performed to determine *P* value. (**E - G**) eYFP transcript detection based library from Supp. Fig. 7 was used to generate UMAP plots showing a feature plot for *Pecam1* (*CD31), Cdh5*, *Prox1, Flt4 (VEGFR3)* and *Pdpn1* (*Podoplanin1)* as known endothelial or lymphatic endothelial cell markers.

Supplemental Figure IX: Expression of adipocyte progenitor markers among UMAP transcriptomic clusters. (**A**) eYFP transcript detection based library from Supp. Fig. 7 was used to generate dot plot analysis depicting the expression levels and percentages of cells expressing a pre-determined list of traditional marker genes relevant for adipocyte progenitor cell types in each cluster. (**B**) Color-coded UMAP plot for integrated libraries based on eYFP transcript detection depicting 25 clusters. (**C-D**) UMAP plots showing feature plots for *Dpp4, Pi16, Ly6a (Sca1), Pdgfrα and Cd9.* (**D**)

The UMAP plots depicting *Pdgfrα and Cd9* are merged to reveal cells expressing both genes.

Supplemental Table I: Differential gene expression analysis of scRNAseq dataset comparing all cells or cluster by cluster.

Supplemental Table II: Sequences of RT-PCR primers used in this study.

SUPPLEMENTAL FIGURES

Supplemental Fig. I:

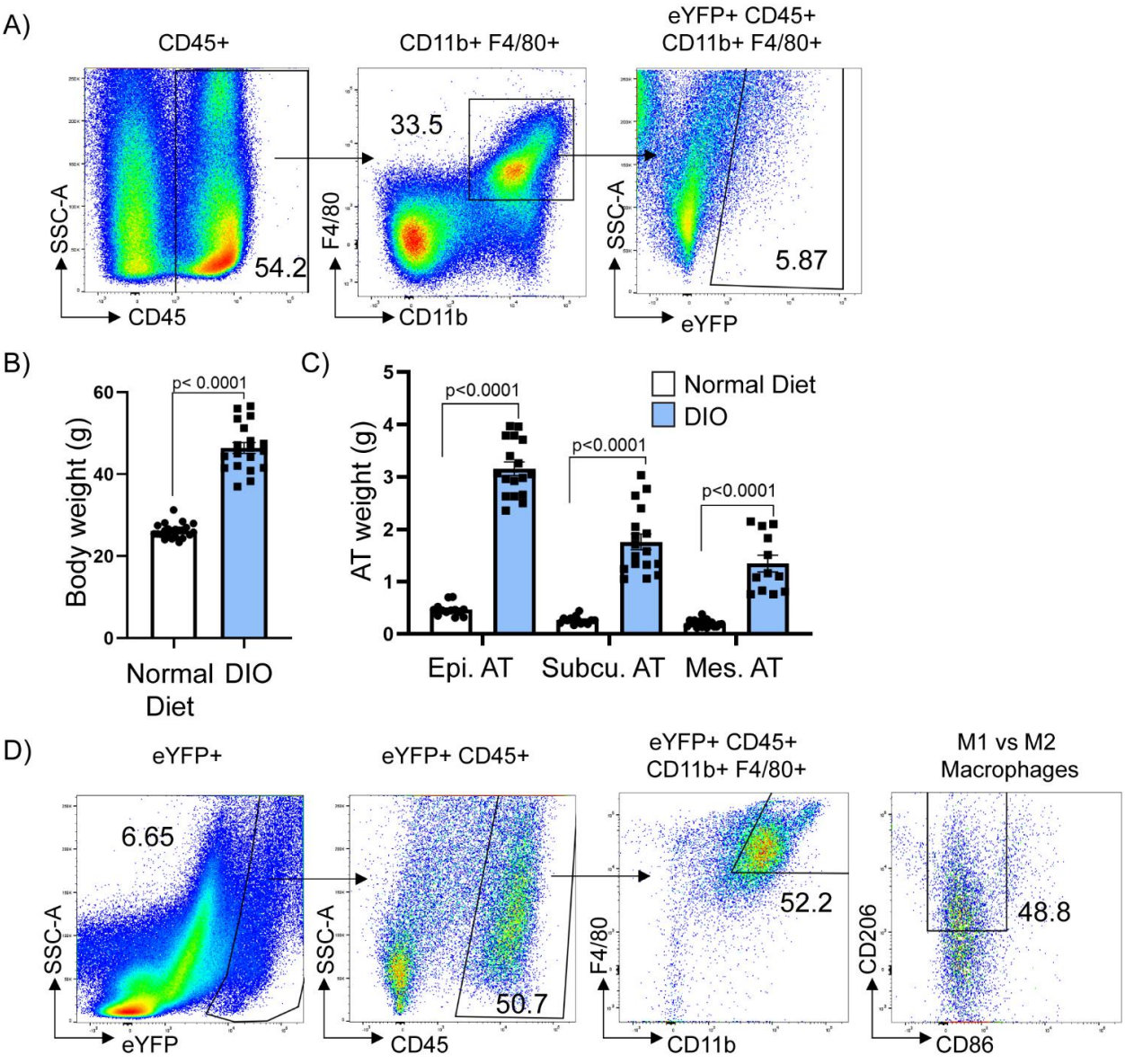

Supplemental Fig. II:

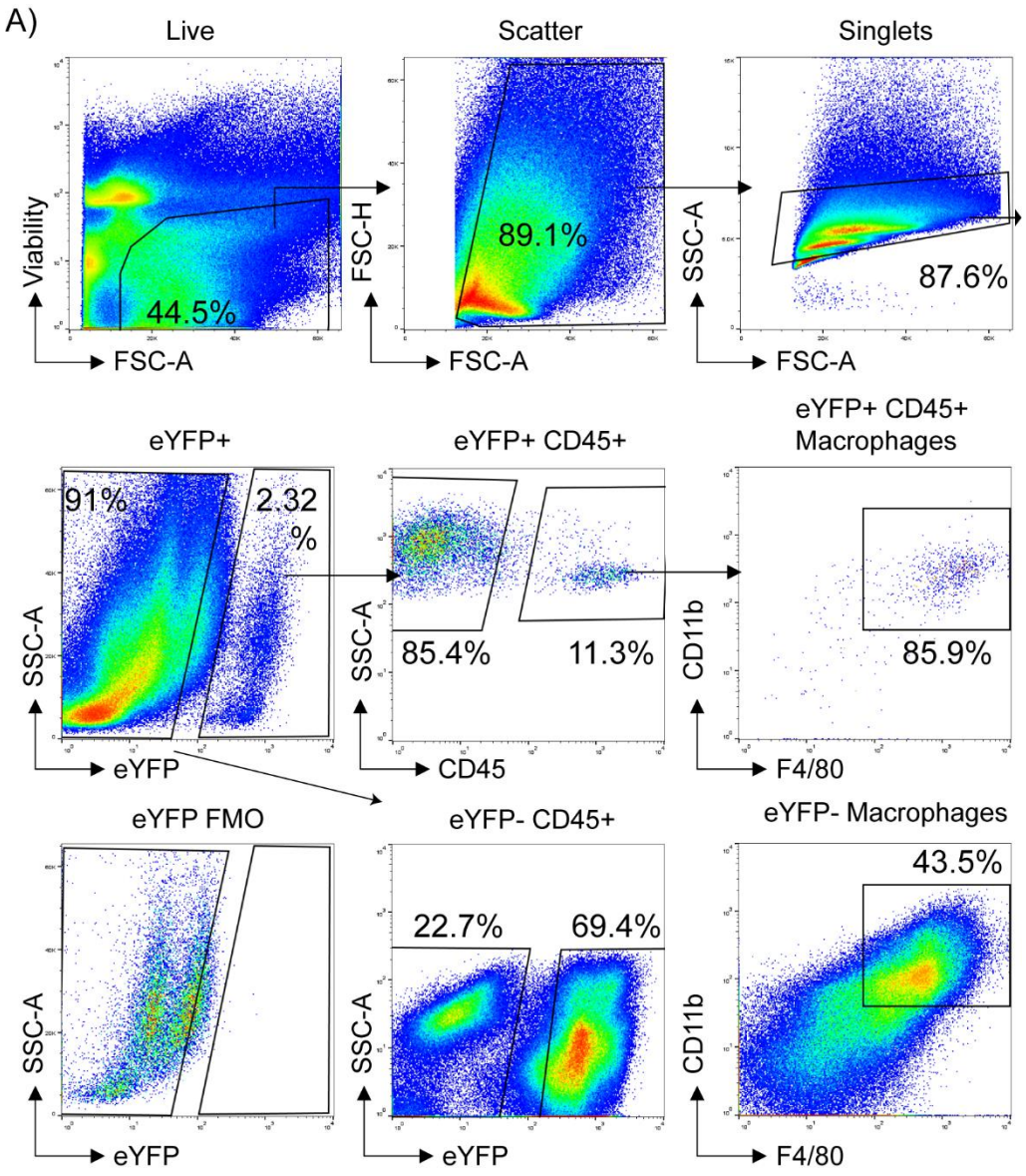

Supplemental Fig. III:

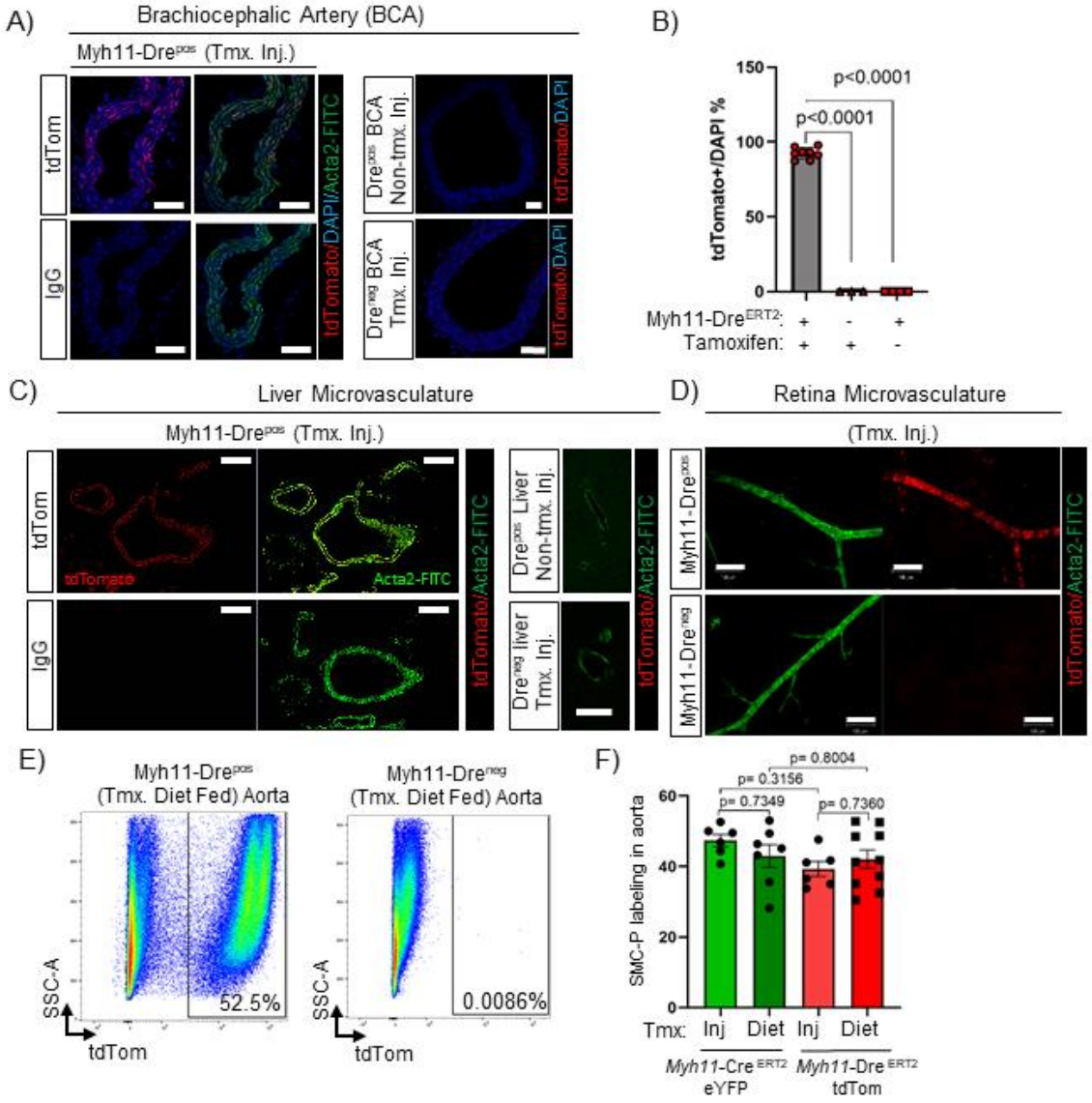

Supplemental Fig. IV:

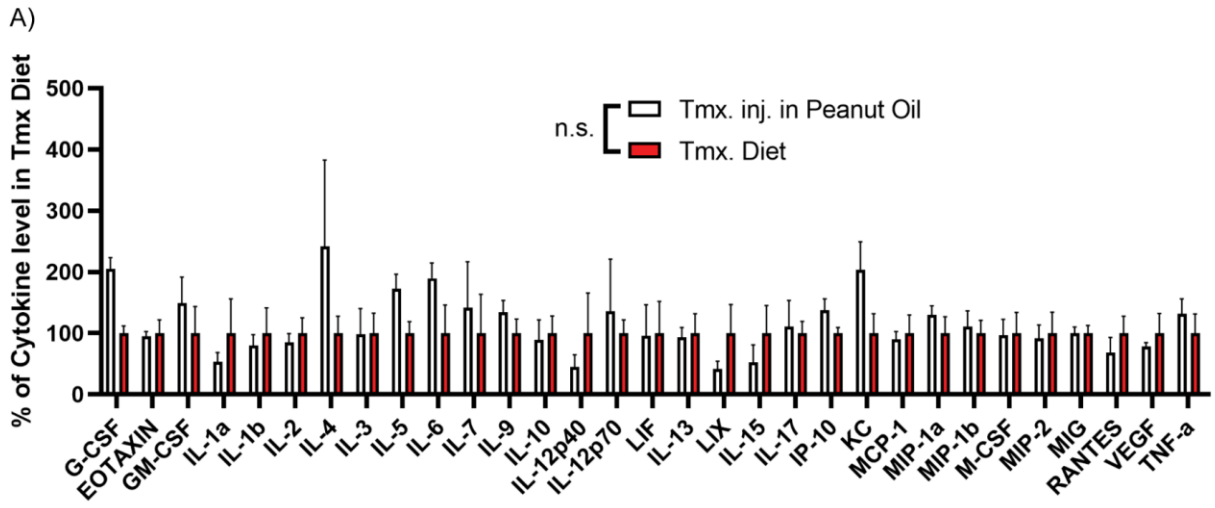

Supplemental Fig. V:

A)

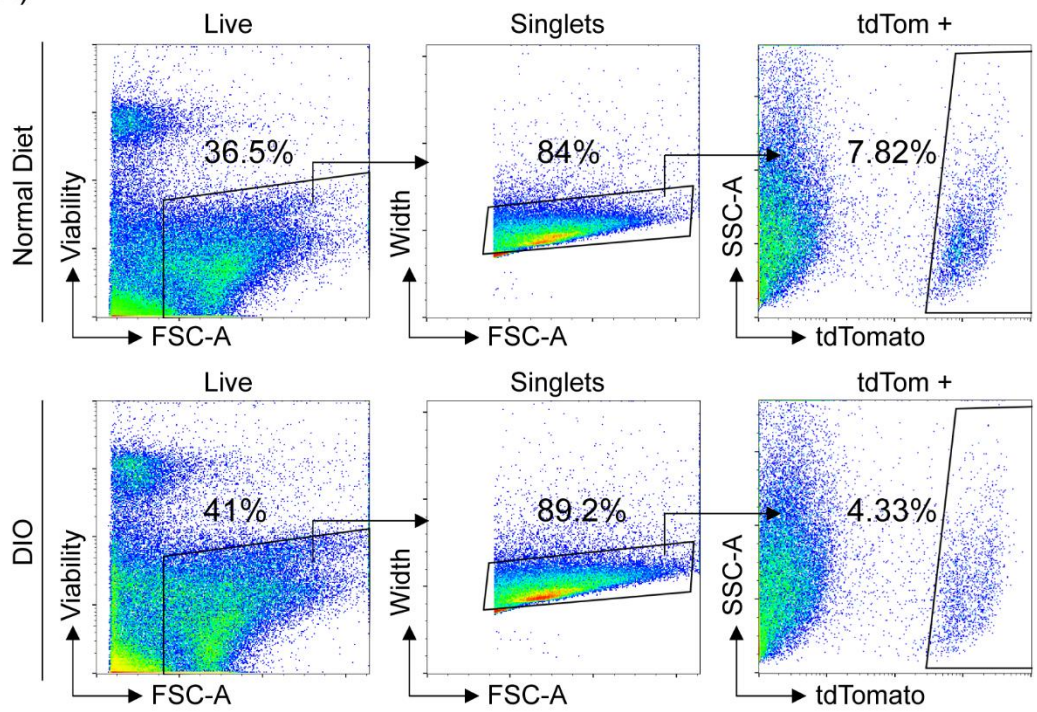

Supplemental Fig. VI:

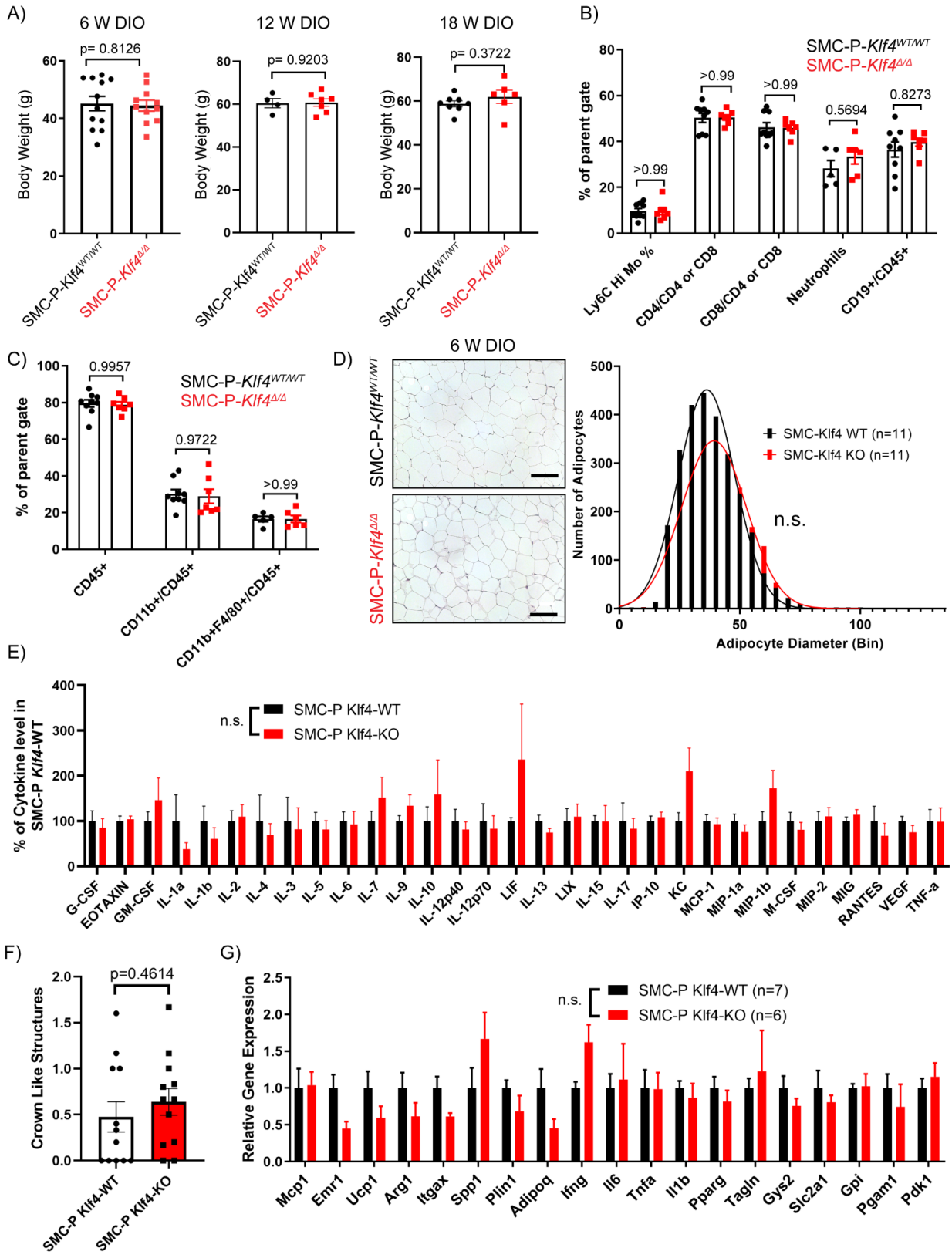

Supplemental Fig. VII:

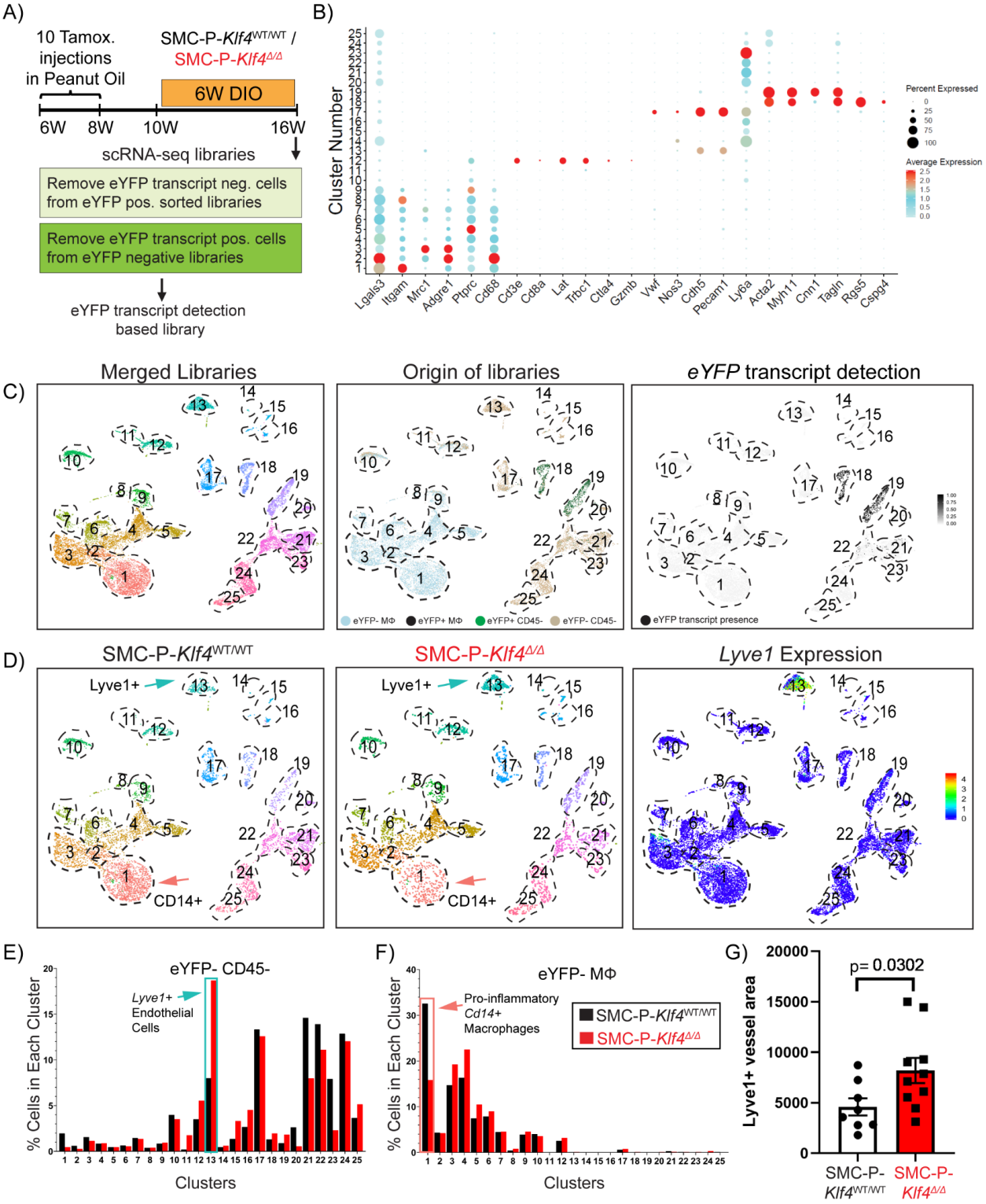

Supplemental Fig. VIII:

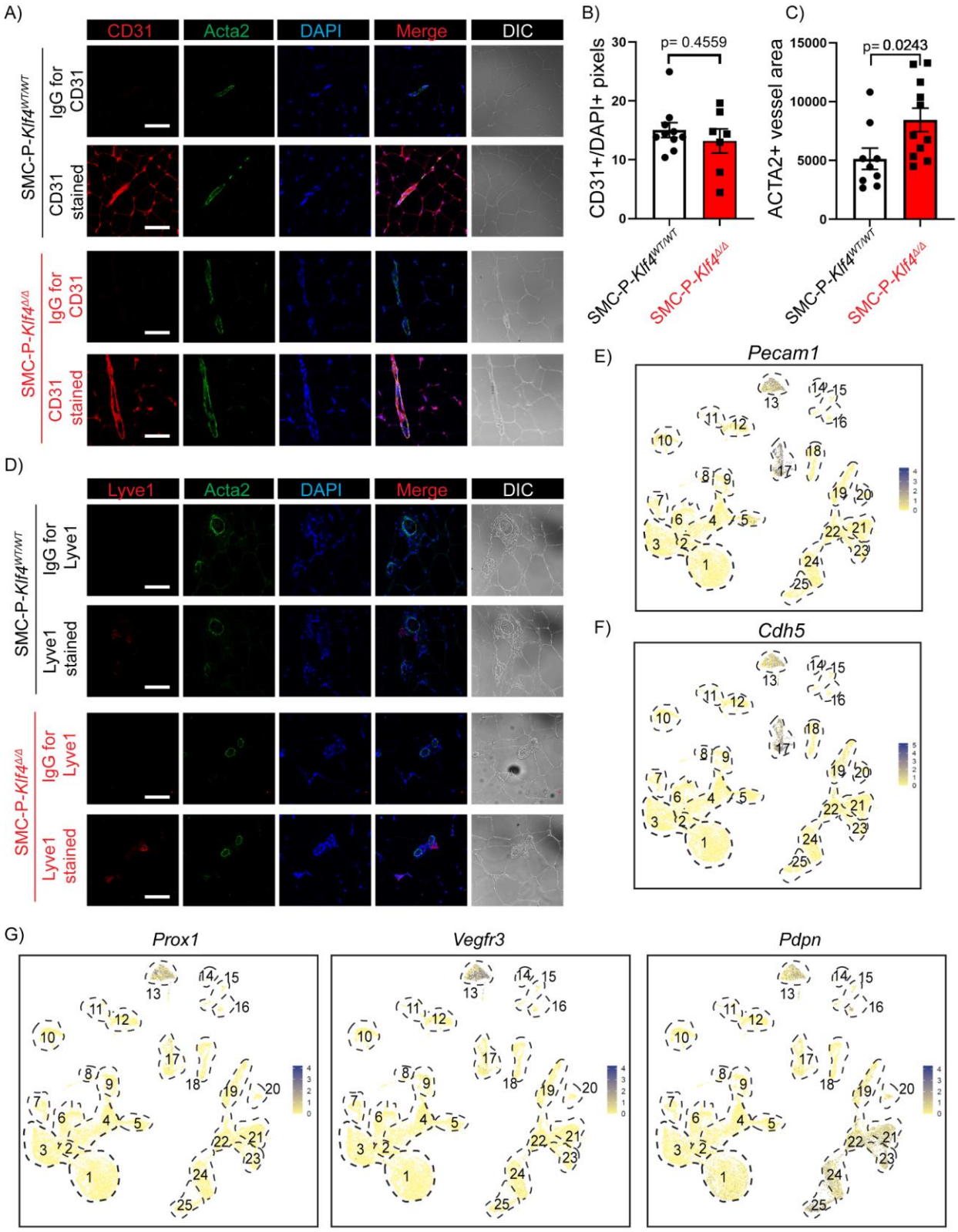

Supplemental Fig. IX:

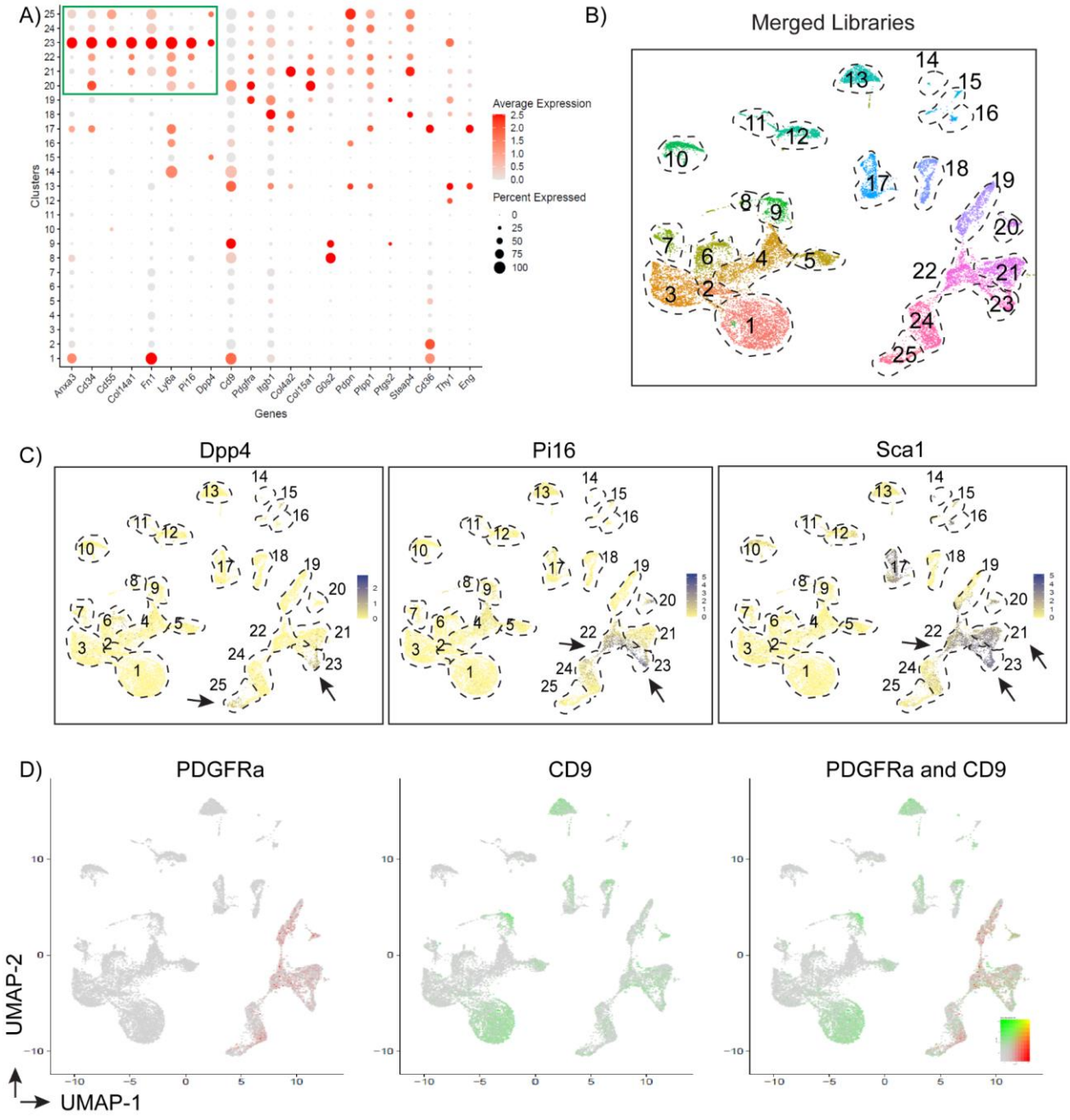

Major Resources Table

Genetically Modified Animals

	Species	Vendor or Source	Background Strain	Other Information	Persistent ID / URL
Transgenic lineage tracing	Mouse	Owens lab (Ref. Shankman et al[1])	C57/Bl6	*Myh11* Cre^{ERT2} Rosa eYFP	Contact corresponding author
Transgenic lineage tracing	Mouse	Owens lab (Ref. Haskins et al[2])	C57/Bl6	*Myh11* Cre^{ERT2} Rosa eYFP *Klf4* $^{Fl/WT}$	Contact corresponding author
Transgenic lineage tracing	Mouse	Owens lab (Ref. Alencar and Owsiany et al[3])	C57/Bl6	*Myh11* Dre^{ERT2}	Contact corresponding author
Inducible Reporter	Mouse	Jackson Labs	C57/Bl6	RosaTomGFP	https://www.jax.org/strain/026931

Animal Breeding

Mouse line	Male	Female
Myh11 Cre^{ERT2} Rosa eYFP	*Myh11* Cre^{ERT2+} Rosa $eYFP^{+/+}$	*Myh11* Cre^{ERT2-} Rosa $eYFP^{+/+}$
Myh11 Cre^{ERT2} Rosa eYFP *Klf4* $^{Fl/WT}$	*Myh11* Cre^{ERT2+} Rosa $eYFP^{+/+}$ *Klf4* $^{Fl/WT}$	*Myh11* Cre^{ERT2-} Rosa $eYFP^{+/+}$ *Klf4* $^{Fl/WT}$
Myh11 Dre^{ERT2} Rosa TomGFP	*Myh11* Dre^{ERT2+} Rosa $TomGFP^{+/+}$	*Myh11* Dre^{ERT2-} Rosa $TomGFP^{+/+}$
Myh11 Dre^{ERT2} Rosa TomGFP	*Myh11* Dre^{ERT2-} Rosa $TomGFP^{+/+}$	*Myh11* Dre^{ERT2+} Rosa $TomGFP^{+/+}$

Antibodies

Target antigen	Vendor or Source	Catalog #	Working concentration	Persistent ID / URL
RFP	Rockland Labs	600-401-379	1:100	https://rockland-inc.com/store/Antibodies-to-GFP-and-Antibodies-to-RFP-600-401-379-O4L_24299.aspx
Acta2-FITC	Sigma Aldrich	F3777	1:500	https://www.sigmaaldrich.com/catalog/product/sigma/f3777?lang=en&region=US
CD31	Abcam	ab124432	1:500	https://www.abcam.com/cd31-antibody-ab124432.html

Lyve1	Abcam	ab33682	1:50	https://www.abcam.com/lyve1-antibody-ab33682.html
CD45-BV650	Biolegend	103151	0.75 ul/ 50 ul	https://www.biolegend.com/en-us/products/brilliant-violet-650-anti-mouse-cd45-antibody-11987
CD45-PE	Biolegend	103106	0.3 ul/ 50 ul	https://www.biolegend.com/en-us/products/pe-anti-mouse-cd45-antibody-100
F4/80 PE-Cy7	Biolegend	123114	0.75 ul/ 50 ul	https://www.biolegend.com/en-us/products/pe-cyanine7-anti-mouse-f4-80-antibody-4070
CD14-PE	Biolegend	150105	0.5 ul/ 50 ul	https://www.biolegend.com/en-us/products/pe-anti-mouse-cd14-antibody-15675
CD11b-PerCP Cy5.5	Biolegend	101228	0.5 ul/ 50 ul	https://www.biolegend.com/en-us/products/percp-cyanine5-5-anti-mouse-human-cd11b-antibody-4257
CD3-PerCP	BD	553067	0.625 ul/ 50 ul	https://www.bdbiosciences.com/eu/applications/research/t-cell-immunology/th-1-cells/surface-markers/mouse/percp-hamster-anti-mouse-cd3e-145-2c11/p/553067
CD31-PerCP Cy5.5	Biolegend	102420	0.312 ul/ 50 ul	https://www.biolegend.com/en-us/products/percp-cyanine5-5-anti-mouse-cd31-antibody-6668
CD31-BV510	BD	563089	1.5 ul/ 50 ul	https://www.bdbiosciences.com/eu/applications/research/stem-cell-research/cancer-research/mouse/bv510-rat-anti-mouse-cd31-mec-133/p/563089
CD86-PerCP	Biolegend	105026	1.5 ul/ 50 ul	https://www.biolegend.com/en-us/products/percp-anti-mouse-cd86-antibody-4277
CD206-BV785	Biolegend	141729	0.625 ul/ 25 ul	https://www.biolegend.com/en-us/products/brilliant-violet-785-anti-mouse-cd206-mmr-antibody-12013
Ly6G-PerCP Cy5.5	Biolegend	127616	0.5 ul/ 50 ul	https://www.biolegend.com/en-us/products/percp-cyanine5-5-anti-mouse-ly-6g-antibody-6116
Ly6C-BV421	Biolegend	128031	0.5 ul/ 50 ul	https://www.biolegend.com/en-us/products/brilliant-violet-421-anti-mouse-ly-6c-antibody-8586
eBioscience™ Fixable Viability Dye eFluor™ 780	Invitrogen	65-0865-14	2 ul/ 50 ul	https://www.thermofisher.com/order/catalog/product/65-0865-14?SID=srch-srp-65-0865-14#/65-0865-14?SID=srch-srp-65-0865-14

Sytox Blue	Invitrogen	S34857	Dilute 1:100, then use 20 ul/ 2M cells	https://www.thermofisher.com/order/catalog/product/S34857#/S34857
LIVE/DEAD™ Fixable Red Dead Cell Stain Kit, for 488 nm excitation	Thermo Fisher	L34972	1:1000	https://www.thermofisher.com/order/catalog/product/L34972#/L34972
CD11b-APC	Biolegend	101212	0.5 ul/ 50 ul	https://www.biolegend.com/en-us/products/apc-anti-mouse-human-cd11b-antibody-345
CD19-BV711			0.75 ul/ 50 ul	
CD4-PE Cy5.5	eBioscience	35-0042-82	0.625 ul/ 50 ul	https://www.thermofisher.com/antibody/product/CD4-Antibody-clone-RM4-5-Monoclonal/35-0042-82
CD8-PE Cy7	Biolegend	100722	0.625 ul/ 50 ul	https://www.biolegend.com/en-us/products/pe-cyanine7-anti-mouse-cd8a-antibody-1906
UltraComp eBeads™ Compensation Beads	Thermo Fisher	01-2222-42	2 drops/ sample	https://www.thermofisher.com/order/catalog/product/01-2222-42#/01-2222-42

Diet

Diet Type	Cat #	Information	Persistent ID / URL
Tamoxifen red diet 40mg -	Envigo TD.130856	Feed instead of Chow diet for 2 weeks and add soft tamoxifen diet 3 times/week	https://www.envigo.com/tamoxifen-custom-diets
Standard Laboratory Diet	Envigo- Teklad 7912	Teklad LM-485 mouse/rat sterilizable diet (irradiated)	https://www.envigo.com/rodent-traditional-natural-ingredient-diets
Diet induced obesity diet (DIO)	Research Diets Inc NC0004611	D12492/ 60% Blue Obesity Diet	https://researchdiets.com/formulas/d12492

Data & Code Availability

Description	Source / Repository	Persistent ID / URL
Myh11 Cre^{ERT2} Rosa eYFP (6W Chow vs 6W DIO) scRNAseq		Code and GEO available upon request
Myh11 Cre^{ERT2} Rosa eYFP $Klf4^{Fl/WT}$ (WT vs KO) 6W DIO scRNAseq		Code and GEO available upon request
Myh11 Cre^{ERT2} Rosa eYFP $Klf4^{Fl/WT}$ (WT vs KO) Mesentery Bulk RNAseq		Code and GEO available upon request

Myh11 Dre^{ERT2} tdTom (6W Chow vs 6W DIO) scRNAseq		Code and GEO available upon request

REFERENCES

1. Shankman, L. S. *et al.* KLF4-dependent phenotypic modulation of smooth muscle cells has a key role in atherosclerotic plaque pathogenesis. *Nat. Med.* (2015). doi:10.1038/nm.3866

2. Haskins, R. M. *et al.* Klf4 has an unexpected protective role in perivascular cells within the microvasculature. *Am. J. Physiol. Circ. Physiol.* (2018). doi:10.1152/ajpheart.00084.2018

3. Alencar, G. F. *et al.* The Stem Cell Pluripotency Genes Klf4 and Oct4 Regulate Complex SMC Phenotypic Changes Critical in Late-Stage Atherosclerotic Lesion Pathogenesis. *Circulation* (2020). doi:10.1161/CIRCULATIONAHA.120.046672